

Observations of Gamma-ray Bursts with the Rossi X-ray Timing Explorer

Hale Bradt¹, Alan M. Levine¹, Francis E. Marshall², Ronald A. Remillard¹,
Donald A. Smith³, and Toshi Takeshima^{2,4}

¹ Massachusetts Institute of Technology, Cambridge MA 02139-4307, USA, Room 37-587; bradt@mit.edu

² Code 662, Goddard Space Flight Center, NASA, Greenbelt MD 20771, USA

³ 2477 Randall Laboratory, University of Michigan, Ann Arbor MI 48109, USA

⁴ Present address: NASDA, Tokyo, Japan 105-8060

Abstract. The role of the Rossi X-ray Timing Explorer (RXTE) in the study of Gamma-ray Bursts (GRBs) is reviewed. Through April 2001, the All-Sky Monitor (ASM) and the Proportional Counter Array (PCA) instruments have detected 30 GRBs. In 16 cases, an early celestial position was released to the community, sometimes in conjunction with IPN results. The subsequent optical and radio searches led to the detection of 5 x-ray afterglows, to at least 6 optical or radio afterglows, to 3 of the 17 secure redshifts known at this writing, and to 2 other likely redshifts. The decay curves of early x-ray afterglows have been measured. The rapid determination of the location of GRB 970828 and the absence of optical afterglow at that position gave one of the first indications that GRBs occur in star-forming regions [6]. The location of GRB 000301C led to the determination of a break in the optical decay rate [16] which is evidence for a jet, and to variability in the optical light curve that could represent gravitational lensing [7]. X-ray light curves of GRB from the ASM in conjunction with gamma-ray light curves exhibit striking differences in different bands and may reveal the commencement of the x-ray afterglow [18].

1 Introduction

The Rossi X-ray Timing Explorer (RXTE) [2] has played a highly significant role in the explosive growth of GRB studies in the afterglow era. The RXTE contributions have been possible because of its ability to rapidly point to a new target, the sensitivity and high-energy response (2 – 60 keV) of the PCA [9], and the wide-field position-determining capability of the ASM [11]. This overview encompasses work through April 2001.

2 Observations of afterglows with the PCA

Searches for early x-ray afterglows with the PCA have been accomplished mostly by means of rapid pointings (few hours) of RXTE that direct the PCA FOV toward the near real time BATSE “Locburst” position, when the position has uncertainty less than a few degrees. In addition early GRB positions from the ASM, BeppoSAX, and the Interplanetary Network (IPN) have been used as

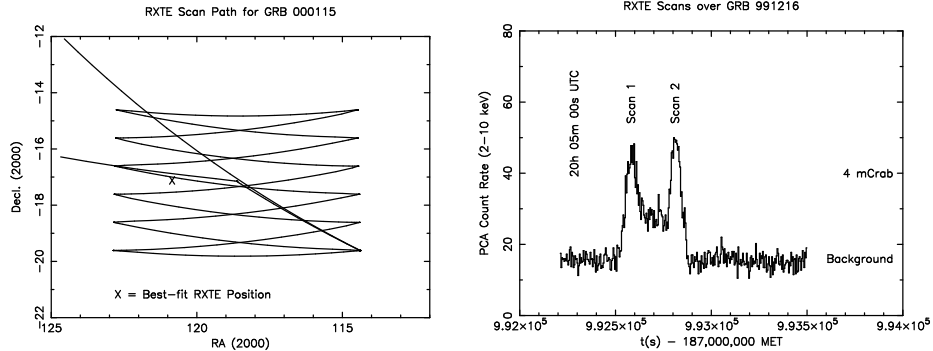


Fig. 1. Typical raster scans by RXTE PCA. Left: the scan track used for GRB 000115. Right: PCA counting rate vs. time for the raster scan of GRB 991216

targets. Raster scans of the region with the 1.0 deg (FWHM) PCA field of view are used to carry out the search; a detection usually can be localized to a few arc minutes; Fig. 1. Such searches by the RXTE/PCA are dependent on the schedule of upcoming command contacts, and upon the burst location relative to the current celestial pointing direction of RXTE. The PCA typically reached its target within a few hours after notification of the burst location.

Table 1. PCA detections of x-ray afterglows

GRB	BATSE peak flux $\text{cm}^{-2} \text{ s}^{-1}$ (50 – 300 keV)	PCA flux @ 3 h (mCrab)	X-ray decay index ^a	Comments ^b
970616*		0.5		3σ PCA detection
970828*		1.0	1.6	See Table 2
990506*	19	3	0.9	Radio; no opt afterglow; host at $z = 1.3$
991216*	68	8	1.8	Opt. and radio afterglow; jet in ISM, $z > 1.02?$
000115*	57	2	1.9	No opt. afterglow

^a Spectral indices are from PCA data alone.

^b See references elsewhere in this report and also on J. Greiner web page:
<http://www.aip.de/~jcg/grbgen.html>

* Prompt position notice provided to community

There have been 31 attempts to view x-ray afterglows with the PCA. Of these 24 were triggered by BATSE Locburst notices and 7 by one or more of the RXTE/ASM, BeppoSAX, and the IPN. Five x-ray afterglows were detected,

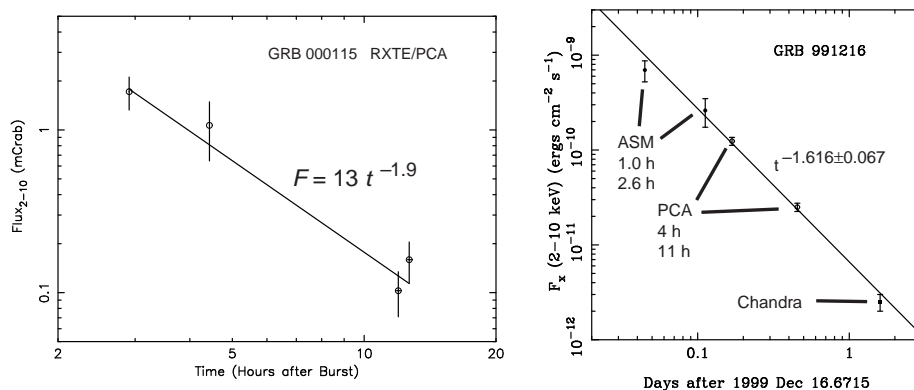


Fig. 2. X-ray decay light curves from RXTE. Left: PCA determination of index for GRB 000115. Right: ASM/PCA/Chandra decay of GRB 991216, reported in Halpern et al. [8]

four derived from Locburst and one from the ASM; Table 1. In each case celestial positions were promptly reported to the community. Highlights of PCA detections and follow-on measurements are:

- Radio afterglow in GRB 990506, but with no optical [19]; host galaxy has $z = 1.3$ [1].
- Optical afterglow in GRB 991216 with a break in the decay curve indicating a jet in interstellar medium [8], radio emission [4], and a reported lower-limit to the redshift, $z > 1.02$ [20].
- X-ray decay indices of 4 bursts; see Table 1 and Fig. 2.

3 Observation of GRBs with the ASM

The ASM, with an instantaneous field of view of ~ 3000 sq. deg. and $\sim 40\%$ duty cycle, has upon occasion serendipitously observed a burst in the FOV of one of its three Scanning Shadow Cameras (SSCs). A detection in a single camera yields a line of position of a few arc minutes by a few degrees. Such an error region can be reduced with IPN lines of position or with PCA scans. Less frequently, a GRB is detected in both of the two azimuthal cameras that have overlapping FOVs (~ 300 sq. deg.). This yields crossed lines of position and an error region of order 10 sq arc min. This is sufficient for radio and optical searches, though PCA or IPN results can further refine the position.

The rate of GRB detection in the overlapping FOVs was initially expected to be ~ 1 per year. The actual rate (see “2-SSC” events in Tables 2 and 3) turns out to be about twice this because (1) the x-ray portion of the bursts tends to be longer than the gamma-ray portion and (2) the ASM rotates every 100 s which shifts the FOVs 6° on the sky. This shift can bring a FOV onto a long-duration burst. It can also bring a camera onto a burst that had just been observed with the other azimuthal camera, thus providing crossed lines of position.

In 5.2 years of operation, up to the present (April 2001) a total of 27 probable GRBs have been detected in the ASM. Of these 24 are confirmed as GRBs by gamma-ray detectors on other satellites; Table 2. Ten of these were detected in 2 SSCs and three were located in a recent global reprocessing of the entire data base. The ASM also recorded at least three other events for which there has been no reported gamma burst from other satellites; Table 3. Each of the listed events has a hard x-ray spectrum, is at high galactic latitude, and is a one-time detection. Thus they could be x-ray bright GRBs. Two of these appear to be afterglow detections as no fast variability is apparent during the 100-s ASM exposures.

The ASM has been providing rapid celestial positions to the community since the commencement of the afterglow era in 1997; to this date 12 such positions have been reported, sometimes in conjunction with IPN reports. Of these, four were observed in two cameras and hence yielded small uncertainties in two dimensions.

The nearly continuous telemetry stream from RXTE, via the TDRSS satellites, makes possible rapid position determinations, in principle less than an hour and in practice usually within a few hours of the burst occurrence time in the RXTE detectors. The events were typically confirmed as due to GRBs in near real time by a BATSE event and thus could be released rapidly with high confidence, well before IPN positions became available. In one case, GRB 970828, the ASM position determination made possible acquisition of the burst by the PCA only 3.6 h after the burst occurrence at RXTE.

The ASM positions have led to 5 optical afterglows and 2 to 4 redshifts. The range in the latter number depends upon the confidence in the determined redshift and the role the ASM played in instigating the search. As noted, the one-camera detections required other information (IPN, SAX, or PCA) to permit fruitful optical and radio searches. In the case of GRB 991216, the ASM did not catch the burst itself, but did capture the early afterglow at 1.0 h and 2.6 h after the burst. The PCA measured the afterglow of this same burst at 4 h and 11 h. Together with a Chandra observation, these provided an excellent measure of the very early x-ray decay of a GRB [8]; Fig. 2. Notable accomplishments that stemmed from ASM results are:

- No optical afterglow was detected in GRB 970828 possibly due to its occurring in a star forming region [6]. Variability in the x-ray afterglow decay was found with ASCA [21].
- Redshifts were obtained for the host galaxy of GRB 980703 ($z = 0.966$) [3] and for the afterglow of GRB 000301C ($z = 2.04$) [10]
- The optical afterglow decay of GRB 000301C showed a clear break [16] and remarkable rapid optical variability on time scales of $\sim 1/2$ day [17] [12] suggestive of a microlensing event [7].
- The x-ray afterglows of GRB 960524 and GRB 991216 were measured by the ASM only 25 min and 1.0 h after the burst, respectively (see above).
- Coincident x-ray (ASM) and gamma-ray light curves of 15 GRBs show marked differences between low and high energies; Fig. 3.

Table 2. ASM detections of confirmed GRBs

GRB ^a	Confirming satellite ^b	Comments ^{c,d}
960228	k	2 SSCs; found in reprocessing
960416	b k u	2 SSCs; soft intermediate x-ray peak; extended x-ray tail
960524	b	2 SSCs; afterglow in ASM 25 min. after burst, fnd. in reproc.
960529	k	2 SSCs
960610	b	2 SSCs; found in reproc.
960727	k u	1 peak; extended x-ray tail
961002	k u	1 peak; extended x-ray tail
961019	b k u	Delayed x-ray peak; x-ray tail
961029	k	Limited x-ray data
961216	b k	Poor ASM position
961230	u	2 SSCs; weak x ray
970815*	b k s u	2 SSCs; strong tertiary x-ray peak
970828*	b k o u	2 SSCs; no opt. afterglow; $z = 0.958?$, $0.33?$ (x-ray line); rad.?
971024*	b k	Weak; position uncertain
971214*	b k n s u	Single longer x-ray peak; OT; $z = 3.42$ from BSAX position
980703*	b k u	2 SSCs; OT; $z = 0.966$; long γ/x tails; radio
981220*	k s u	8 Crab (5–12 keV); γ peaks smeared in x rays
990308*	b k u	OT; host galaxy underluminous or distant
991216	b n u	OT; x-ray afterglow at opt. pos. at 1.0 h, 2.6 h (ASM)
000301C*	k n u	3 Crab (5–12 keV); OT; $z = 2.04$; rapid opt. var. (lensing?)
000508*	b u	2 Crab; emerged from earth occultation
001025*	n u	~ 4 Crab (5–12 keV); no optical
010126*	k n u	~ 5 Crab (5–12 keV); no optical
010324*	s u	2 SSCs; det. 360 s after GRB onset; no det. rapid var. in ASM, but decays factor of 4 in 100 s (afterglow?); no opt.

^a The GRBs detected in 1996 were located in archival searches.^b b=BATSE; k=KONUS; n=NEAR; o=SROSS-C; s=BSAX; u=Ulysses^c See refs. herein and on J. Greiner: <http://www.aip.de/~jcjg/grbgen.html>^d OT = optical transient

* Prompt position notice provided to community

Table 3. ASM GRB not confirmed by gamma detectors

Date	α, δ^a (J2000)	Start (MJD) (interval)	I_{max} (mC)	Gal. lat.	Comments
961225	154.97, 64.04	50442.2620 (>90s)	360	+46°	2 SSCs; flat l.c.; afterglow?
970123	184.68, -21.20	50471.0707 (>190 s)	62	+41°	2 SSCs; ramping down; afterglow?
000913	16.355, -16.008	51800.6711	700	-78°	

^a $\sim 90\%$ errors: 0.2° for the first two bursts. For the third: line length = 2.50° , line width = 0.090° , pos. angle = -36.930°

4 Coincident x/gamma light curves

The ASM provides light curves for GRB detections in three x-ray energy bands: 1.5 – 3 keV, 3 – 5 keV, and 5 – 12 keV. In addition, the ASM time series data mode may reveal temporal variability in each channel down to a time resolution of 0.125 s if the GRB is the dominant x-ray source in a camera’s FOV. These data provide valuable information in a band not typically monitored by gamma-ray experiments. (But note, e.g., the x-ray detections of GRBs (< 10 keV) with Ginga [14] and with the currently operational WFC on BeppoSAX [5].)

The ASM in conjunction with gamma-ray detectors on BATSE, BeppoSAX, Ulysses, Konus, and NEAR have yielded multifrequency light curves over the range 1.5 to >300 keV. Fifteen of these have been collected and analyzed by Smith et al. [18]. They show diverse morphologies with striking differences between the x-ray and gamma-ray bands; Fig. 3. For example, the pronounced 3rd ASM peak of GRB 970815 is not detected in the upper BATSE energy bands. This peak could represent the beginning of the afterglow in the external shock model [13]. This supposition is supported by (1) the ~ 8 -s delay of the peak time in the highest ASM energy channel (~ 7 keV) relative to that of the lowest channel (~ 2.25 keV) and (2) the achromatic decay of this peak, with decay indices in each of the 3 ASM energy channels consistent with $\alpha = 1.3 \pm 0.1$.

Smith et al. [18] also studied the durations of gamma bursts as a function of energy and compared them with the $E^{-0.5}$ power law expected from an origin in synchrotron radiation [15]. Examples that match well are the two distinct peaks of GRB 960416 taken separately (Figs. 3, 4a,b) and the single peak (see [18]) of GRB 000301C (Fig. 4h). The more complex bursts (see light curves in [18]) are not consistent with this prediction. Some have flatter curves which widen more slowly than expected with decreasing energy; Fig. 4c,d. Other complex bursts show a flat curve at high energies but an excess at low energies; Fig. 4e,f. These inconsistencies are probably indicative of complex interactions that violate the assumption of a single infusion of energy followed by cooling through radiation.

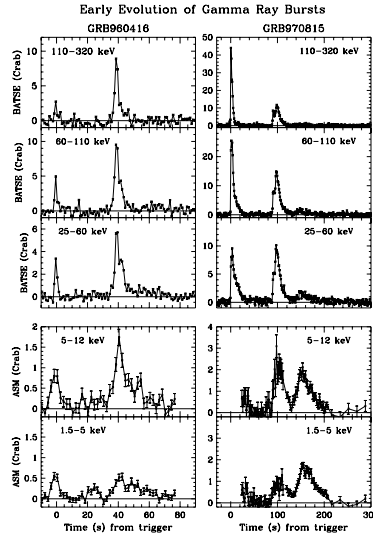


Fig. 3. Light curves in 3 BATSE energy bands and 2 ASM bands of GRB 960416 and GRB 970815, from Smith et al. [18]

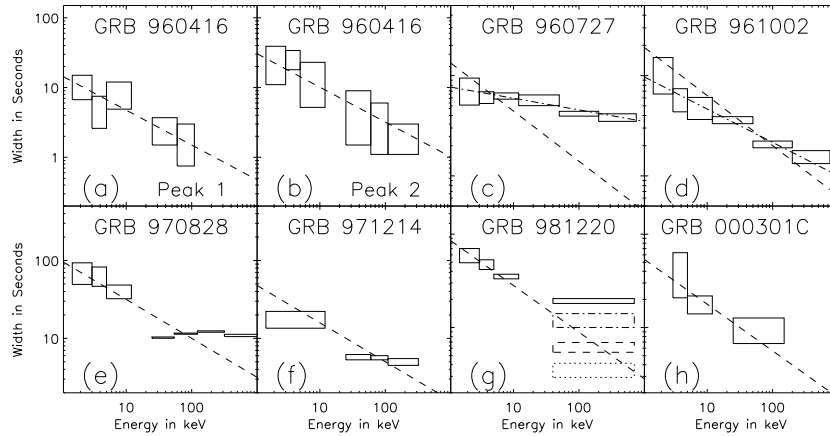


Fig. 4. Peak width vs. energy for seven GRBs. The dashed lines indicate a logarithmic slope of -0.5 , from Smith et al. [18]

5 RXTE burst studies in the HETE era

The RXTE will continue to contribute occasional additional positions, light curves, and decay indices of GRBs with increased reliance on ASM self-triggered events and on IPN crossing lines of positions and confirmations, now that BATSE is no longer in orbit. Most important, the RXTE/PCA has the unique potential to acquire a HETE burst extremely rapidly, say within 1/2 hour of the burst and to study the temporal activity in the afterglow with high statistics, a domain not heretofore explored.

Acknowledgments

We acknowledge the contributions of the many individuals on the ASM and PCA teams, the observers whose data are included in Fig. 3, and NASA for the continued operation of RXTE.

References

1. J. S. Bloom, D. A. Frail, R. Sari: AJ, in press (2001, astro-ph 0102371; see Table 1)
2. H. V. Bradt, R. E. Rothschild, J. H. Swank: A&AS **97**, 355 (1993)
3. S. G. Djorgovski, S. R. Kulkarni, J. S. Bloom, R. Goodrich, D. A. Frail, L. Piro, E. Palazzi: ApJ **508**, L17 (1998)
4. D. A. Frail, et al.: ApJ **538**, L129 (2000)
5. F. Frontera, et al.: ApJS **127**, 59 (2000)
6. P. J. Groot et al.: ApJ **493**, L27 (1998)
7. P. M. Garnavich, A. Loeb, K. Z. Stanek: ApJ **544**, L11 (2000)
8. J. P. Halpern, et al.: ApJ **543**, 697 (2000)
9. K. Jahoda, J. H. Swank, A. B. Giles, M. J. Stark, T. Strohmayer, W. Zhang, E. H. Morgan: Proc. SPIE, **2808**, 59 (1996)
10. B. L. Jensen et al.: A&A, in press (astro-ph 0005609)
11. A. M. Levine, H. Bradt, W. Cui, J. G. Jernigan, E. H. Morgan, R. Remillard, R. E. Shirey, D. A. Smith: ApJ **469**, L33 (1996)
12. N. Masetti et al.: A&A **359**, L23 (2000)
13. P. Meszaros, M. Rees: ApJ, **476**, 232 (1997)
14. Y. Ogasaka, T. Murakami, J. Nishimura, A. Yoshida, E. E. Fenimore: ApJ **383**, L61 (1991)
15. T. Piran: Phys. Rep., 314(6), 575 (1999, astro-ph 9810256):
16. J. E. Rhoads, A. S. Fruchter: ApJ **546**, 117 (2001)
17. R. Sagar, V. Mohan, S. B. Pandey, A. K. Pandey, C. S. Stalin, A. J. Castro Tirado: Bull. Astr. Soc. India **28**, 499 (2000)
18. D. A. Smith et al. 2001: ApJ, submitted (astro-ph 0103357)
19. G. B. Taylor, J. S. Bloom, D. A. Frail, S. R. Kulkarni, S. G. Djorgovski, B. A. Jacoby: ApJ, **537**, L17 (2000)
20. P. M. Vreeswijk, et al.: GCN Circ. 496 (1999)
21. A. Yoshida, M. Namiki, C. Otani, N. Kawai, T. Murakami, Y. Ueda, R. Shibata, S. Uno: AdSpR **25**, 761 (2000)